

Supplementary Information

**Sulfobetaine methacrylate-functionalized graphene oxide-IR780
nanohybrids aimed for improved breast cancer phototherapy**

Miguel M. Leitão^a, Cátia G. Alves^a, Duarte de Melo-Diogo^{a,*}, Rita Lima-Sousa^a,
André F. Moreira^a, Ilídio J. Correia^{a,b,*}

^a CICS-UBI – Centro de Investigação em Ciências da Saúde, Universidade da Beira Interior, 6200-506 Covilhã, Portugal.

^b CIEPQPF – Departamento de Engenharia Química, Universidade de Coimbra, 3030-790 Coimbra, Portugal.

* Corresponding Authors E-mail: icorreia@ubi.pt (Ilídio J. Correia) and demelodiogo@fcsaude.ubi.pt (Duarte de Melo-Diogo). Telephone: +351 275 329 055

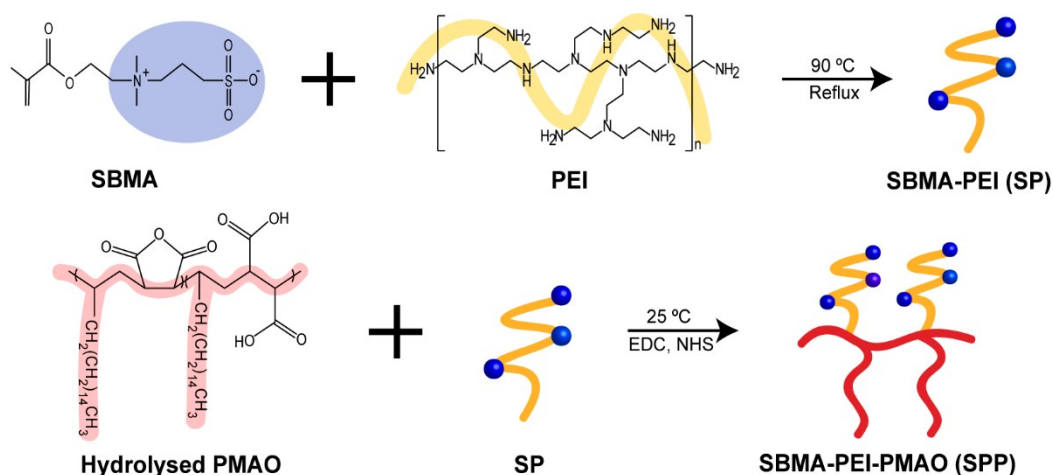


Figure S1. Schematic representation of the SP and SPP synthesis.

FTIR characterization of SP, SPP and PP

The successful synthesis of SBMA-PEI (SP) and SBMA-PEI-PMAO (SPP) was confirmed by FTIR (Figure S2 and S3). The spectrum of SBMA has a peak at 1035 cm^{-1} and 1165 cm^{-1} corresponding to the S=O stretch (Figure S2). In turn, the PEI spectrum displays peaks at $3347\text{--}3280\text{ cm}^{-1}$ (N-H stretch) and 1594 cm^{-1} (N-H bending) - Figure S2 (1, 2). The spectrum of SP presents the SBMA and PEI characteristic peaks, hence confirming the grafting of SBMA into PEI (Figure S2).

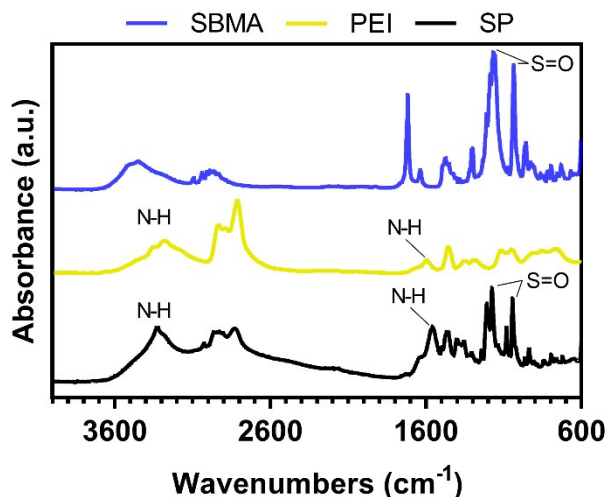


Figure S2. FTIR spectra of SBMA, PEI and SP.

The FTIR spectrum of hydrolysed PMAO displayed its characteristic peaks at 2920 cm^{-1} and 2851 cm^{-1} (C-H stretch) belonging mostly to its alkyl chain, as well as that at 1708 cm^{-1} (C=O stretch) corresponding to the hydrolysed PMAO maleic anhydride ring - (Figure S3) (3). In turn, the FTIR spectrum of SPP presents the hydrolysed PMAO (C-H stretch) and SP (S=O stretch and N-H bending) signature peaks, hence confirming the conjugation of SP to hydrolysed PMAO (Figure S3).

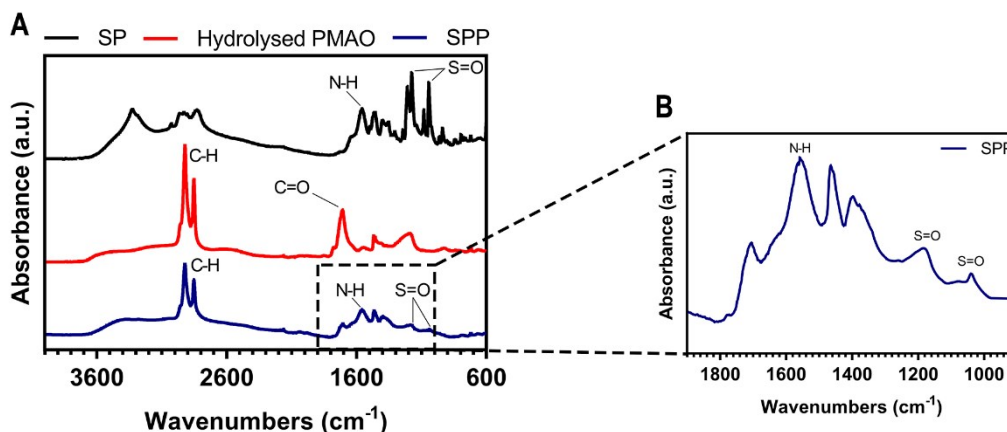


Figure S3. FTIR spectra of SP, hydrolysed PMAO and SPP (A). FTIR spectrum of SPP in the 1900–900 cm^{-1} wavenumber range (B).

On the other hand, the PEI-PMAO (PP) FTIR spectrum displays the characteristic peaks of hydrolysed PMAO (C-H stretch) and of PEI (N-H bending), thereby proving its successful preparation (Figure S4).

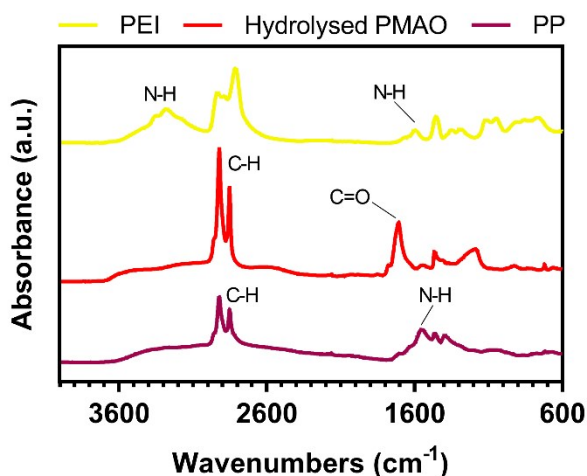


Figure S4. FTIR spectrum of PEI, hydrolysed PMAO and PP.

NMR characterization of SP and SPP

The successful synthesis of SP was confirmed by ^1H NMR (Figure S5). The ^1H NMR spectrum of SBMA displayed the characteristic peaks of its methyl ($\delta \approx 3.2$ ppm ($-\text{N}(\text{CH}_3)_2-$) and methylene ($\delta \approx 3.6$ ppm ($-\text{CH}_2\text{N}(\text{CH}_3)_2-$); $\delta \approx 3.0$ ppm ($-\text{CH}_2\text{SO}_3$) protons (Figure S5) (4). In turn, the spectrum of PEI presented several peaks at $\delta \approx 2.8 - 2.5$ ppm belonging to its methylene protons ($-\text{CH}_2\text{CH}_2-$) (5, 6). The spectrum of SP displays the SBMA and PEI characteristic peaks, hence confirming the grafting of SBMA into PEI (Figure S5).

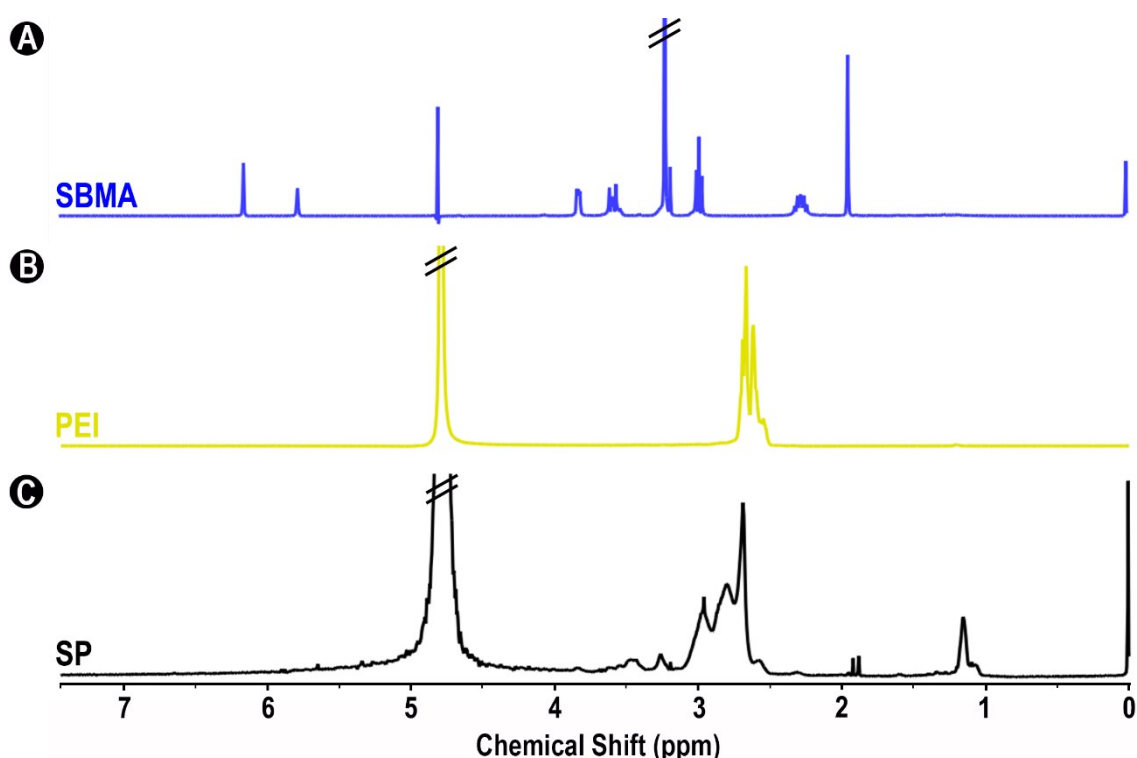


Figure S5. ^1H NMR spectra of SBMA (A; in 9:1 (v/v) $\text{H}_2\text{O}/\text{D}_2\text{O}$), PEI (B; in 9:1 (v/v) $\text{H}_2\text{O}/\text{D}_2\text{O}$) and SP (C; in 9:1 (v/v) $\text{H}_2\text{O}/\text{D}_2\text{O}$).

^1H NMR was also employed to confirm the synthesis of SPP (Figure S6). The spectrum of hydrolysed PMAO presented signals from its methylene ($\delta \approx 1.2$ ppm ($-\text{CH}_2-$) and methyl ($\delta \approx 0.8$ ppm ($-\text{CH}_3$) protons (Figure S6) (3). In the spectrum of SPP, peaks belonging to SP and hydrolysed PMAO protons can be observed, hence confirming the preparation of SPP (Figure S6).

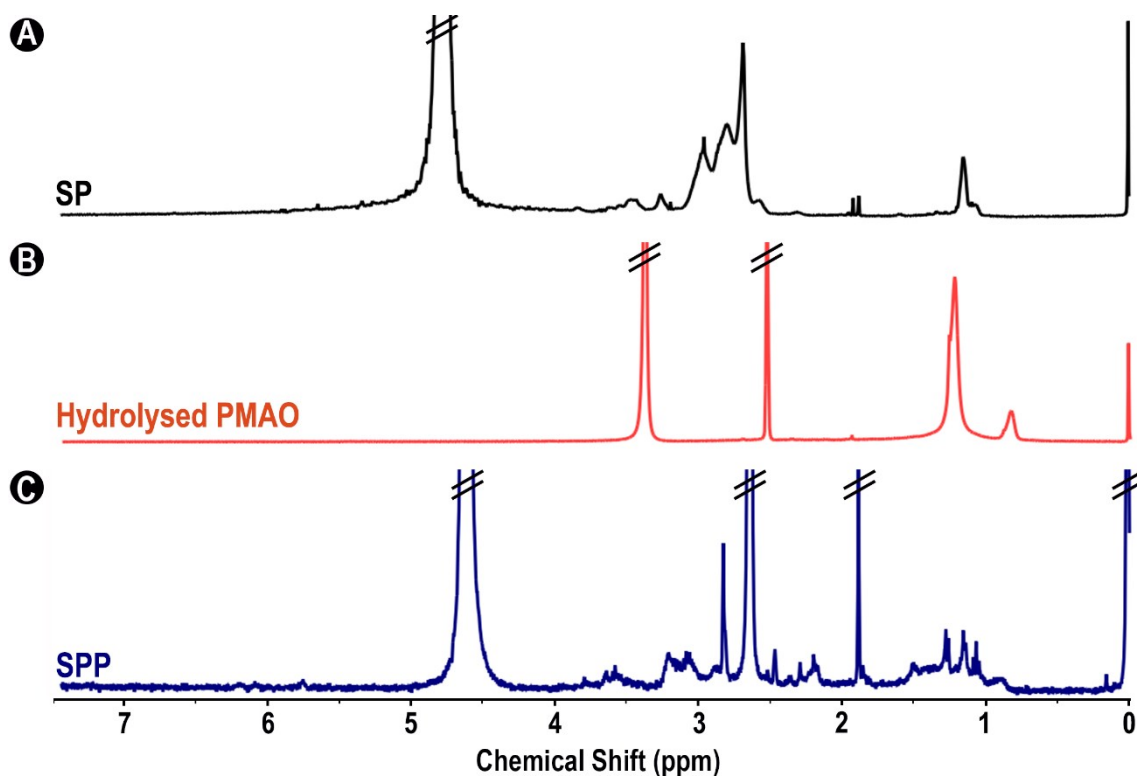


Figure S6. ^1H NMR spectra of SP (A; in 9:1 (v/v) $\text{H}_2\text{O}/\text{D}_2\text{O}$), hydrolysed PMAO (B; in DMSO-d_6) and SPP (C; in 1:1 (v/v) $\text{DMSO-d}_6/(9:1 \text{ (v/v) } \text{H}_2\text{O}/\text{D}_2\text{O})$).

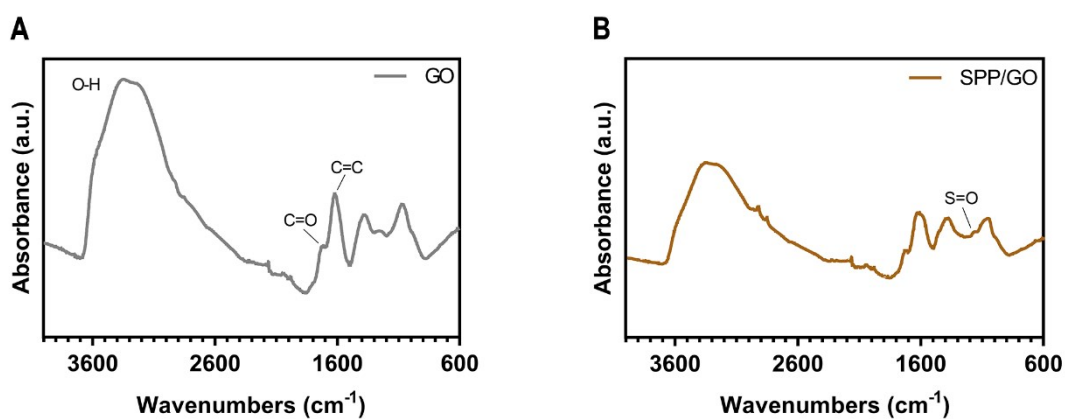


Figure S7. FTIR spectra of GO (A) and SPP/GO (B). The FTIR spectrum of GO displays peaks at 3350, 1715 and 1614 cm^{-1} that are attributed to O-H, C=O and C=C stretches (7), respectively. In the FTIR spectrum of SPP/GO, a peak belonging to S=O (1177 cm^{-1}) is present.

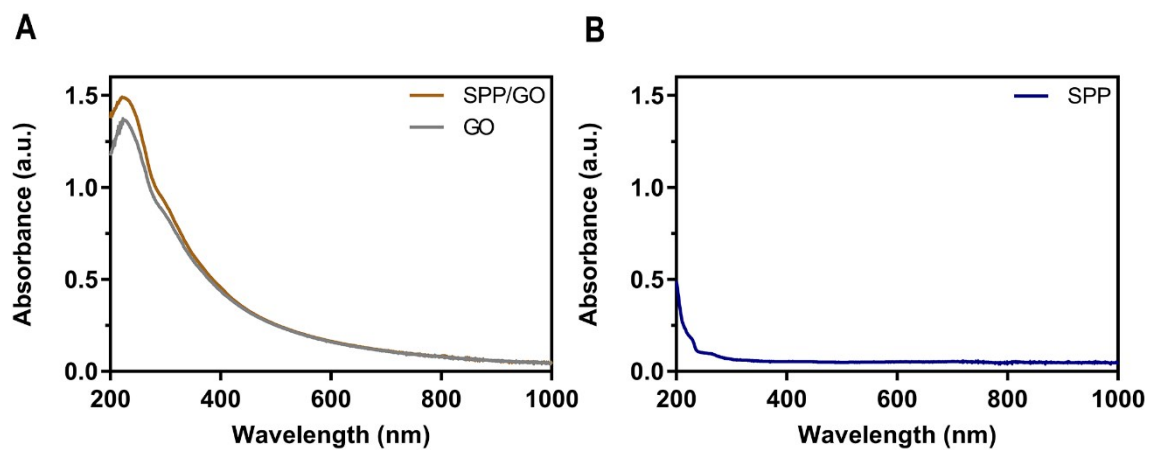


Figure S8. Absorption spectra of SPP/GO and GO (in water) (A). Absorption spectrum of SPP (in methanol) (B).

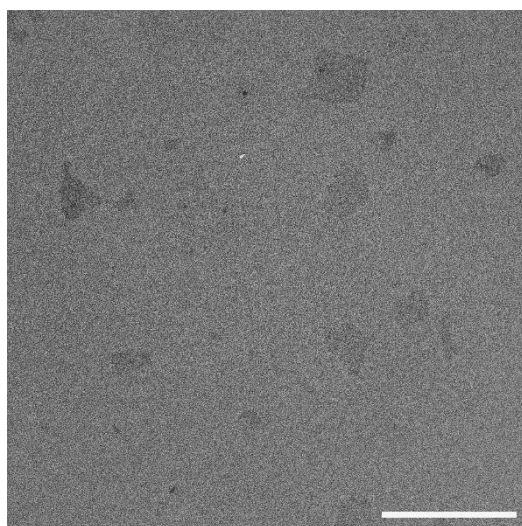


Figure S9. TEM image of SPP/GO. Scale bar corresponds to 500 nm.

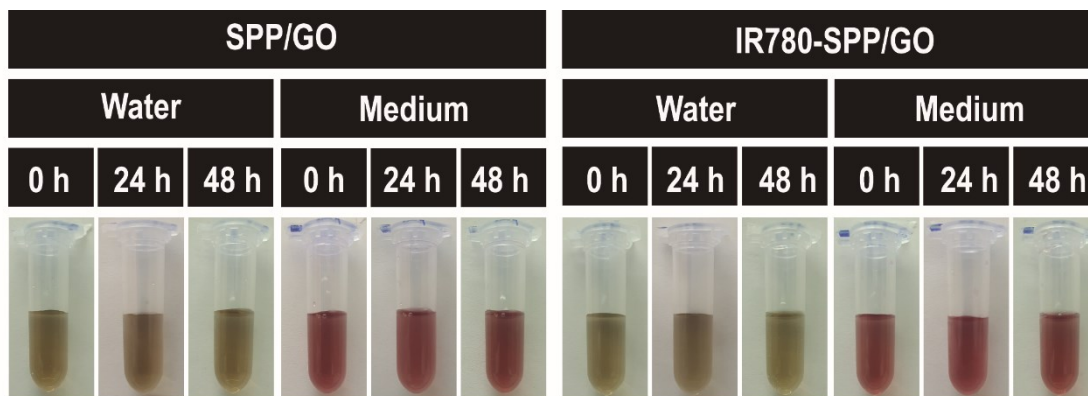


Figure S10. Macroscopic images of SPP/GO and IR780-SPP/GO in water and serum supplemented medium (DMEM-F12 supplemented with FBS (10 % (v/v))), at different time points.

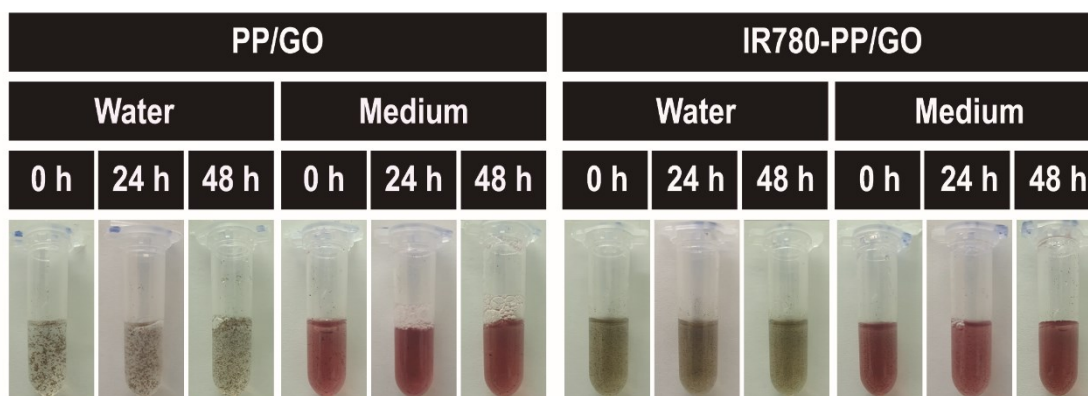


Figure S11. Macroscopic images of PP/GO and IR780-PP/GO in water and serum supplemented medium (DMEM-F12 supplemented with FBS (10 % (v/v))), at different time points.

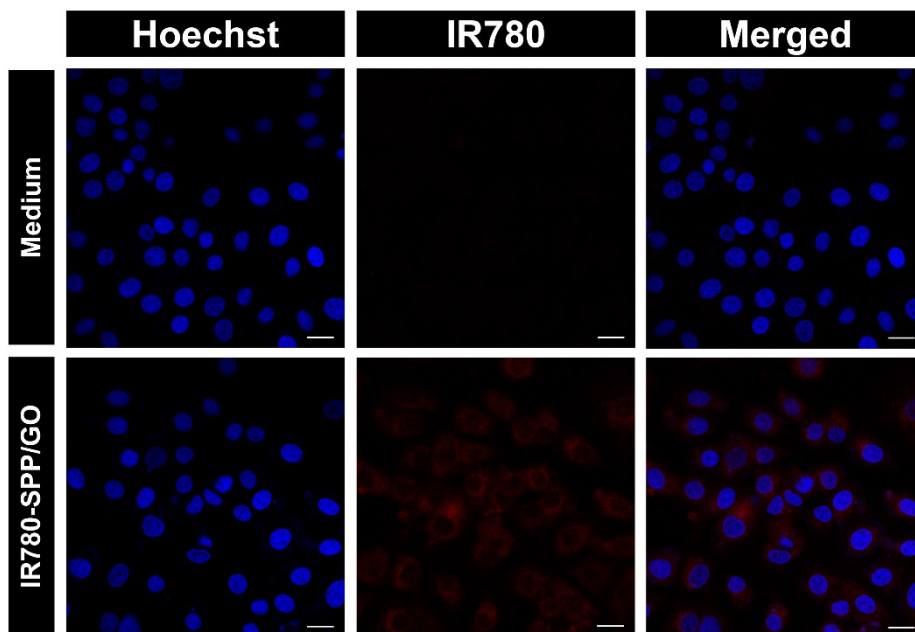


Figure S12. Cellular uptake of IR780-SPP/GO by MCF-7 cells. Cells solely incubated with medium were used as a control. Blue channel: Hoechst 33342[®] stained nucleus; Red channel: IR780. Scale bars correspond to 20 μm .

Supplementary References

1. Luo Z, Qi Q, Zhang L, Zeng R, Su L, Tang D. Branched polyethylenimine-modified upconversion nanohybrid-mediated photoelectrochemical immunoassay with synergistic effect of dual-purpose copper ions. *Analytical Chemistry*. 2019;91(6):4149-56.
2. Huang X, Ishitobi H, Inouye Y. Formation of fluorescent platinum nanoclusters using hyper-branched polyethylenimine and their conjugation to antibodies for bio-imaging. *RSC Advances*. 2016;6(12):9709-16.
3. Lima-Sousa R, de Melo-Diogo D, Alves CG, Costa EC, Ferreira P, Louro RO, et al. Hyaluronic acid functionalized green reduced graphene oxide for targeted cancer photothermal therapy. *Carbohydrate Polymers*. 2018;200:93-9.
4. Alves CG, de Melo-Diogo D, Lima-Sousa R, Correia IJ. IR780 loaded sulfobetaine methacrylate-functionalized albumin nanoparticles aimed for enhanced breast cancer phototherapy. *International Journal of Pharmaceutics*. 2020;582:119346.
5. Wang Y-Q, Su J, Wu F, Lu P, Yuan L-F, Yuan W-E, et al. Biscarbamate cross-linked polyethylenimine derivative with low molecular weight, low cytotoxicity, and high efficiency for gene delivery. *International Journal of Nanomedicine*. 2012;7:693.
6. Zhou B, Shen M, Bányai I, Shi X. Structural characterization of PEGylated polyethylenimine-entrapped gold nanoparticles: an NMR study. *Analyst*. 2016;141(18):5390-7.
7. de Melo-Diogo D, Pais-Silva C, Costa EC, Louro RO, Correia IJ. D- α -tocopheryl polyethylene glycol 1000 succinate functionalized nanographene oxide for cancer therapy. *Nanomedicine*. 2017;12(5):443-56.